Received: 26 February 2023 | Accepted: 1 March 2023 | Published on: 2 April 2023

DOI: 10.1002/ctpp.202300029

ORIGINAL ARTICLE

Contributions to Plasma Physics

Günter Kelbg, the Kelbg potential and its impact on quantum plasma theory

M. Bonitz[1] | W. Ebeling[2] | A. Filinov[1] | W.D. Kraeft[3] | R. Redmer[3] | G. Röpke[3]

[1]Institut für Theoretische Physik und Astrophysik, Christian-Albrechts-Universität zu Kiel, Leibnizstraße 15 24098, Kiel, Germany

[2]Institute of Physics, Humboldt University Berlin, D-12489 Newtonstrasse 15 Berlin, Germany

[3]Institute of Physics, Rostock University, D-18059 Einsteinstraße 23–24 Rostock, Germany

Correspondence
M. Bonitz, Institut für Theoretische Physik und Astrophysik, Christian-Albrechts-Universität zu Kiel, Leibnizstraße 15, 24098 Kiel, Germany.
Email: bonitz@physik.uni-kiel.de

Funding information
Deutsche Forschungsgemeinschaft, Grant/Award Number: BO1366/15-1

Abstract

Günter Kelbg did remarkable early work in the field of quantum statistical physics, in particular for dense quantum plasmas. In 2022 we celebrated his 100th birthday. On this occasion, we give a brief overview of his main scientific achievements in the field of quantum plasmas, complemented by some biographical background of his research and teaching environment at Rostock University. Kelbg's main achievement is the derivation of a regularized quantum pair potential. We demonstrate that it is still of high relevance for molecular dynamics and quantum Monte Carlo simulations of dense plasmas.

KEYWORDS

Kelbg potential, PIMC simulations of hydrogen, quantum plasmas, warm dense matter

1 | INTRODUCTION

Dense quantum plasmas are presently of high relevance in many fields, including the astrophysics of planets and compact stars, for example, References [1, 2] as well as laboratory experiments with high-intensity lasers or free electron lasers. The most striking application is the quest for inertial confinement fusion.[3] To achieve a physical understanding of these systems requires to develop adequate models and computer simulations. For recent overviews, see References [4, 5].

The theory of dense quantum plasmas emerged in the late 1950s and early 1960s. Here an important role was played by Günter Kelbg (Figure 1) and his group at Rostock University in the former German Democratic Republic. In this article we recall the main results of the work of Kelbg, concentrating on the quantum pair potential that he introduced, and illustrate its recent applications in molecular dynamics (MD) and quantum Monte Carlo simulations of dense plasmas as well as the quark-gluon plasma (QGP). We conclude by presenting new path integral Monte Carlo (PIMC) simulation results for dense partially ionized hydrogen where we compare the use of the original Kelbg potential, the improved Kelbg potential[6,7] and the exact solution of the two-particle Bloch equation.

FIGURE 1 Günter Kelbg around 1970, as director of the Institute of Theoretical physics.

2 | KELBG'S LIFE AND MAIN WORKS

In 1949 the University of Rostock appointed Hans Falkenhagen—a former student of Peter Debye and meanwhile a well-known expert in electrolyte theory—to the chair of theoretical physics. Hans Falkenhagen was an impressive personality and gifted teacher. He immediately attracted Rostock the most talented students, including Margarete Leist, Günter Kelbg, Eberhard Gerdes and Hans Jacob, and formed a theoretical and an experimental electrolyte group. A few years later Ernst Schmutzer, Heinz Ulbricht, Heinz Hoffmann and two of the present authors (WE and WDK) joined the theory group. A whole series of PhD dissertations emerged.

When Falkenhagen retired, his successor on the chair of theoretical physics became Günter Kelbg. Kelbg was born on March 26, 1922, in Königsberg (now Kaliningrad)—the son of Gustav Kelbg, who worked as a clerk in a bank in Königsberg, and his wife Marie Kelbg. After finishing school he started to study mathematics and physics at the University of Königsberg. After his service in the army and some time in prison and working in a mine in the north of France, in 1948 he joined again his parents in Güstrow. He continued to study physics and mathematics at Rostock University and finished with a thesis on the "Hill differential equation", his advisor was Prof. Hans Schubert. Then he joined the new group of Hans Falkenhagen. He started research in electrolyte theory and graduated in 1954 with a dissertation on "Deviations from Ohm's law" and published his first papers on the transport theory of charged hard spheres with Hans Falkenhagen and Margarete Leist in "Annalen der Physik", "Elektrochemie" and "Zeitschrift für Physikalische Chemie", see References [8–10]. Then Kelbg turned to the equilibrium statistical thermodynamics of ionic solutions and wrote interesting papers on charges interacting by model potentials possessing a Fourier transform, so-called Kramers-Glauberman-Yukhnovskiy potentials. Further Kelbg got interested in the powerful concepts of collective coordinates in statistical physics that are based on Fourier representations of coordinates, due to Bohm, Pines, Bogolyubov, Zubarev, Yukhnovskiy, and others. In 1959 Günter Kelbg defended his habilitation thesis devoted to the theory of electrolytes with short-range square-well potentials. In 1959 he was appointed docent and in 1961 professor of theoretical physics and started to give lectures. His favourite lecture was Quantum mechanics, where he closely followed the textbook of P.A.M. Dirac "Principles of quantum mechanics." Attending this high-level course were, among others, the late Dietrich Kremp[11] and Klaus Kilimann, as well as two of the present authors (WE and WDK), who also served as Kelbg's teaching assistants. Stimulated by these teaching activities, Kelbg's research interest shifted to quantum effects in Coulomb systems, and in 1963–1964 appeared his first quantum theory publications in "Annalen der Physik." They contained new results for the microfield in a plasma[12] and a fundamental achievement in quantum plasma theory: a new effective interaction potential of Coulomb interacting particles which is now connected with his name—the Kelbg potential which he presented in a series of three papers, cf. References [13–15]. He showed that the effective interaction between charges in a quantum plasma is given by a rather complicated expression which we give here only in a simplified form, which is commonly called Kelbg-Deutsch potential,

FIGURE 2 Günter Kelbg 1972 on the occasion of his 50th birthday, surrounded by his co-workers and the staff of his office. On the r.h.s are Heinz Hoffmann and two of the present authors.

cf. References [13, 14, 16–19],

$$V_{ij}^K(r) = \frac{e_i e_j}{r}\left[\left(1-\exp\left(-\frac{r}{\lambda_{ij}}\right)\right) \pm \frac{\delta_{ij}}{2}\exp\left(-\frac{r}{\lambda_{ij}}\right)^2\right]; \qquad \lambda_{ij} = \frac{\hbar}{\sqrt{2m_{ij}k_BT}}, \tag{1}$$

where the last term is an exchange correction for identical particles, and λ_{ij} is the thermal De Broglie wavelength (m_{ij} denotes the reduced masses of particles i and j), which is proportional to the square root of the inverse temperature. This potential is related to the Kramers-Glauberman-Yukhnovskiy model which Kelbg studied for applications to electrolytes. Among the most important properties of the new potential is that it is finite at zero inter-particle distance, $V_{ij}^K(0) = \frac{e_i e_j}{\lambda_{ij}}$, (except for identical particles with parallel spin), and approaches the Coulomb potential, for large distances. The origin of this behaviour is an elementary quantum diffraction effect giving rise to a finite extension of the wave function of the interacting particles and, hence, to a finite pair interaction energy.

As another topic, a favourite mathematical method of Kelbg was collective coordinates, which he used for the derivation of thermodynamic properties of quantum plasmas. In this field, he came again across the work of Ihor R. Yukhnovskiy, well-known Ukrainian scientists from Lviv University, who visited Rostock in 1968 where he started a close collaboration and developed a friendship with members of the Rostock group. Kelbg's work was always performed on the highest mathematical level. He was a brilliant expert on all known special functions of mathematical physics with his favourite functions being the generalized hyper-geometric functions. A running joke among his coworkers was that Kelbg was able to solve any hard problem of theoretical physics by reducing it to hyper-geometric functions. After the retirement of Hans Falkenhagen in 1961 Günter Kelbg took over the directorship of the Institute of Theoretical Physics, and in 1979 he became director of the department of (all) physics institutions at the University of Rostock. Kelbg formed a strong theory group consisting of many co-workers. Some of them are shown in Figure 2 at a meeting dedicated to his 50th birthday in 1972. Subsequently, Statistical physics in Rostock evolved into a center of high international reputation attracting well-known guests such as Igor Yukhnovskiy (Lviv), Harold Friedman (Stony Brook), Jan Stecki (Warsaw), Yuri Klimontovich (Moscow), and others, see Figure 3. In the last years of his life, Günter Kelbg had been elected among others into positions in the local politics of the city of Rostock, where he was fighting for more democratic structures. He passed away on January 26, 1988, in Rostock and did not witness the democratic changes of the fall of 1989.

3 | DERIVATION AND PROPERTIES OF THE KELBG POTENTIAL

The approach of Kelbg is based on the thermodynamic equilibrium density matrix of interacting particle pairs of species a, b, the diagonal elements of which defines the binary Slater sums, $S_{ab}^{(2)}$,

$$S_{ab}^{(2)}(\mathbf{r}_1, \mathbf{r}_2) = \left\langle \mathbf{r}_1\mathbf{r}_2 \left| \hat{\rho}_{ab} \right| \mathbf{r}_1\mathbf{r}_2 \right\rangle \quad . \tag{2}$$

FIGURE 3 The school of Günter Kelbg (front row, 3rd from the right) around 1974 with visiting Harold Friedman (Stony Brook, in the center, next to Kelbg) and Jan Stecki (Warsaw, far left). At the far right are Hartmut Krienke and Rainer Sändig. Second and third left are Werner Ebeling and Heinz Ulbricht. Also pictured are (second row) Wolf-Dietrich Kraeft, Dietrich Kremp, Klaus Kilimann and Jürgen Einfeldt.

Here, the species a and b are charges ($a, b \in \{++, --, -+, +-\}$). The average pair potential (PP), that is, the potential of two charges in vacuum, is given by

$$V_{ab}^{\mathrm{PP}}(r_1, r_2) = -k_B T \ln S_{ab}^{(2)}(r_1, r_2)\,. \tag{3}$$

We will show, that this concept leads indeed, in first approximation, to expression (1). While the concept of Slater sums was introduced earlier by Slater and Morita, a detailed investigation and its application to Coulomb systems are due to Kelbg, cf. References [13, 16, 20, 21].

An explicit result can be obtained for low densities. Then the pair density operator is given by

$$\hat{\rho}_{ab} = \exp\left(-\beta \hat{H}_{ab}\right) \quad , \quad \hat{H}_{ab} = -\frac{\hbar^2}{2m_{ab}}\Delta + V_{ab} \quad ,$$

where $\hat{H}_{ab}$ is the Hamiltonian of the relative motion of the pair, with the reduced mass m_{ab}. In his derivation, Kelbg proceeded by introducing a plane wave representation and defining an operator in Fourier space $\mathbf{k}$:

$$W_{ab}(\beta, \mathbf{k}) = \exp\left(-\beta \hat{H}_{ab}\right) \exp(+i\mathbf{k}\cdot\mathbf{r}) \quad . \tag{4}$$

Differentiating with respect to β yields the Bloch equation which reads, for two interacting particles,

$$\frac{\partial W_{ab}}{\partial \beta} = \frac{\hbar}{2m_{ab}}\Delta W_{ab} - V_{ab} W_{ab} \quad , \tag{5}$$

which is solved by iteration. The first order in e^2 leads to a solvable diffusion problem with a source term. Solving this equation and, including symmetry effects for fermions, one obtains, to first order (linear in e^2) in Fourier space of relative

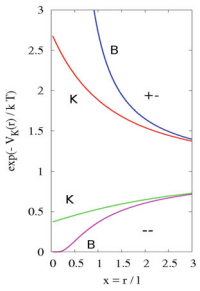

FIGURE 4 Exponent of the Kelbg potential (K)—the first nonlinear approximation to the pair Slater sum—for pairs of opposite and equal charges, respectively, compared to the classical Boltzmann approximation (B) for hydrogen at $T = 10{,}000$ K. The large differences at small distances are due to Heisenberg uncertainty and the Pauli exclusion principle, see also Figure 6.

distances.[13,14,22]

$$V_{ab}^{K}(k) = \frac{4\pi e_a e_b}{k^2} \exp\left(-\frac{\lambda_{ab}^2 k^2}{4}\right)_1 F_1\left(\frac{1}{2}, \frac{3}{2}, \frac{\lambda^2 k^2}{4}\right) \pm \delta_{ab} \frac{2k_B T \pi e_a e_b \lambda_{ab}^2}{(2s_a + 1)} \times \exp\left(-\frac{\lambda_{ab}^2 k^2}{4}\right)_2 F_2\left(\frac{1}{2}, \frac{1}{2}, \frac{3}{2}, \frac{3}{2}, \frac{\lambda_{ab}^2 k^2}{4}\right), \tag{6}$$

where k is a wavenumber, and ${}_1F_1$ and ${}_2F_2$ are the well-known generalized hyper-geometric functions. Here the first (main) term has been given already in Kelbg's pioneering work written in 1963, Reference [13], whereas the second one was added in 1967 in References [16, 22]. Approximating the ${}_1F_1$—function by $1/\left(1 + \lambda^2 k^2\right)$ and ${}_2F_2$ by $\exp\left(-\lambda^2 k^2\right)$, returning to (relative) coordinate space, one arrives indeed at the Kelbg-Deutsch potential (1). This simple potential is graphically rather similar to the full potential and is shown in Figure 4. Its most important property is the removal of the divergence of the Coulomb potential at zero distance. In fact, this potential has the limit

$$V_{ij}^{k}(r \to 0; T) = \frac{e_i e_j}{\lambda_{ij}(T)} \sim \text{sign}\left(e_i e_j\right) T^{1/2}. \tag{7}$$

This is a very intuitive result: while for point particles the pair potential diverges, for quantum particles with a finite extension λ, the charge is distributed over a finite volume resulting in a finite value of the interaction at zero distance. When the temperature is lowered, this extension increases, and the value of the potential approaches zero.

For the derivation of the exact low-density thermodynamics, one needs the full Kelbg potential (6), as shown in Reference [22]. The derivation of his potential may be indeed considered the pioneering contribution of Günter Kelbg to dense plasma theory since this potential is still actively used in simulations, as we will show in Section 4.

The Kelbg approximation for the pair density matrix is exact only for small $\xi-$ parameters, where $\xi_{ab} = -\left(e_a e_b\right) / \left(k_B T \lambda_{ab}\right)$. A generalization valid also for larger $\xi-$ parameters is

$$\rho_{ij}^{(2)}(\mathbf{r}) = \exp\left[-\beta V_{ij}^{K} - A_{ij}\left(\xi_{ij}\right) \exp\left(-\frac{r^2}{\lambda_{ij}^2}\right)\right], \tag{8}$$

which has been given in References [21, 24]. It has been proven that this expression gives the correct asymptotic at large distances, as well as the correct height and first derivative at $r = 0$. The function $A_{ij}\left(\xi_{ij}\right)$ has been reduced to the exactly known hydrogen wave functions at $r = 0$ and has been tabulated, cf. References [21, 24]. An alternative expression with similar properties will be given in Section 4.3.

We note that Kelbg studied in his seminal work not only the binary Slater sums but also the general N-particle problem, cf. References [13, 15, 20], and his scheme can be applied to any N-particle problem with the Hamiltonian $\mathbf{H}^{(N)} = \mathbf{H}_0 + V$.

Kelbg and Hoffmann found, for the density operator, an expansion with respect to β:

$$\boldsymbol{\rho}^{(N)}(\mathbf{1},\mathbf{2},\ \dots\ ,N) = \frac{\exp(-\beta V)}{Z_0}\left[1+\sum_{n=2}^{\infty}\frac{\beta^n}{n!}f_n\right]\exp(-\beta H_0)\,, \tag{9}$$

and provided a recursion formula for the coefficients f_n and exact expansions of the first terms of the expansion of the density operator and the Slater functions with respect to β, e^2 and $\hbar^2$.[13,14,20] These results were also used in a recent study of the quantum-statistical He-problem, cf. Reference [25].

For PIMC calculations the N-particles density matrix is in most cases expanded in terms of the two-particle density matrix. For this one needs, however, the off-diagonal density matrix which reads[26,27]

$$\rho_{ab}\left(r_a,r'_a,r_b,r'_b\right) = C\exp\left[-\frac{m_a}{2\beta\hbar^2}\left(r_a-r'_a\right)^2\right]\exp\left[-\frac{m_b}{2\beta\hbar^2}\left(r_b-r'_b\right)^2\right]\exp\left[-\beta\Phi\left(r_a,r'_a,r_b,r'_b\right)\right], \tag{10}$$

where

$$\Phi_{ab}\left(r_{ab},r'_{ab}\right) = e_a e_b\int_0^1\frac{d\alpha}{d_{ab}(\alpha)}erf\left[\frac{d_{ab}(\alpha)}{2\lambda_{ab}\sqrt{\alpha(1-\alpha)}}\right], \tag{11}$$

and $d_{ab}(\alpha) = \mid \alpha\mathbf{r}_{ab} + (1-\alpha)\mathbf{r}'_{ab} \mid$. A new detailed derivation and discussion has recently been given in Reference [27]. More details on the use of the Kelbg potential in PIMC simulations are given in Section 4.1.

4 | APPLICATIONS OF KELBG'S POTENTIAL AND FURTHER DEVELOPMENTS

A direct use of the Kelbg potential in plasma theory and simulations is justified only at weak coupling since its derivation involved a perturbation theory in e^2. Nevertheless, this potential has been applied extensively to moderately degenerate quantum plasmas, for example, References [27–30]. Kelbg's concept was also extended to other systems including the interaction of electrons with hydrogen and helium atoms[31] and even to the QGP, see Section 4.2. On the other hand, there have been developed various concepts that allow one to extend the concept of quantum potentials also to stronger coupling. This will be summarized in the following.

4.1 | Application to quantum Monte Carlo simulations of dense hydrogen and electron–hole plasmas

The Kelbg potential has found extensive use in quantum Monte Carlo simulation of dense plasmas developed by V. Filinov and co-workers, cf. References [26, 32–35]. Similarly, simulations were developed by the same group for electron–hole plasmas and liquids in semiconductors, References [36–38], as well as for hole and quantum ion crystals, cf. References [39, 40]. Here the idea of reducing a strongly coupled quantum system to a weakly coupled weakly degenerate system to which the Kelbg potential applies is based on the identity

$$\exp\left(-\beta\hat{H}_{ab}\right) = \left[\exp\left(-\frac{\beta}{P}\hat{H}_{ab}\right)\right]^P, \quad P = 2,3,\ \dots\ , \tag{12}$$

where P denotes the number of high-temperature factors ("imaginary times slices" or "beads"). This gives rise to Feynman's path integral representation of quantum mechanics. The evaluation of thermodynamic averages with products of many high-temperature factors leads to very high-dimensional integrals that are efficiently evaluated with Monte Carlo methods (path-integral Monte Carlo, PIMC). If P is sufficiently large, on the r.h.s. perturbation theory applies, and the Kelbg potential can be used.

An example of the first PIMC simulations of hydrogen of V. Filinov et al. that have used the Kelbg potential is shown in Figure 5. Let us first recall the main dimensionless parameters: the classical and quantum coupling parameters, Γ, r_s

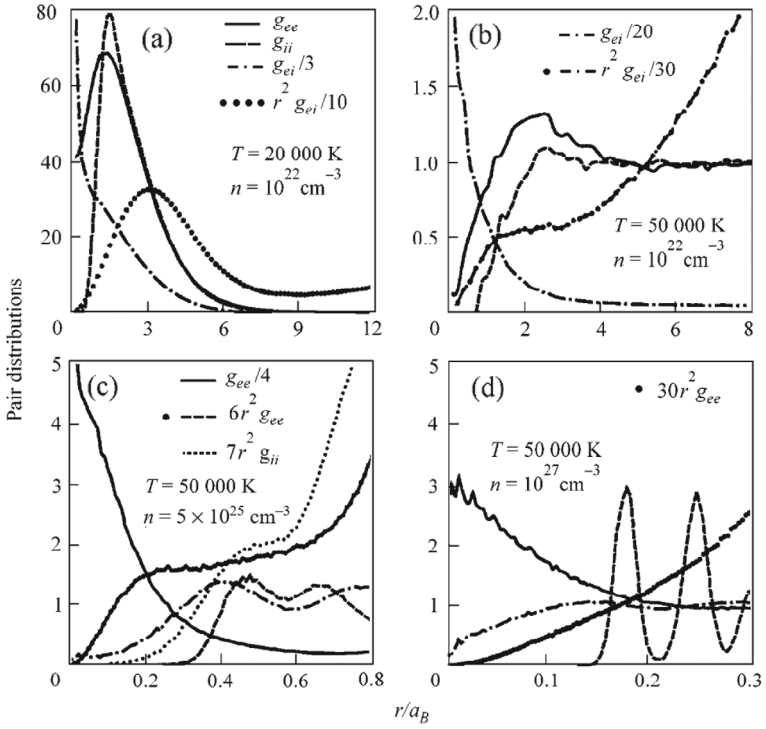

FIGURE 5 Early PIMC result for dense hydrogen that uses the Kelbg potential, Equation (1), for densities and temperatures indicated in the figure. Shown are the pair distributions of electrons (full lines), ions (dashed lines), and of electron-ion pairs (dash–dotted lines). The values for the coupling, degeneracy, and Brueckner parameters are (a) $\Gamma = 2.9$, $\chi = 1.46$, and $r_s = 5.44$; (b) $\Gamma = 1.16$, $\chi = 0.37$, $r_s = 5.44$; (c) $\Gamma = 19.8$, $\chi = 1848$, $r_s = 0.318$; and (d) $\Gamma = 53.8$, $\chi = 37.000$, $r_s = 0.117$. Figure modified from Reference [32].

and the degeneracy parameter χ:

$$\Gamma = \frac{e^2}{\bar{r} k_B T}, \qquad r_s = \frac{\bar{r}}{a_B}, \qquad \chi = n\lambda^3, \qquad \lambda = \frac{h}{\left[2\pi m k_B T\right]^{1/2}}, \tag{13}$$

where $\bar{r}$ is the mean interparticle distance and λ the thermal DeBroglie wavelength of an ideal gas. In case of a multi-component plasma, we replace $\lambda \to \lambda_{ij}$ which involves the reduced mass of particles i and j. Figure 5 shows various states of highly compressed hydrogen. The top row is for a density of 10^{22} cm^{-3}, close to solid state density. The pair distribution functions indicate that the plasma is dominated by atoms and molecules where the fraction of molecules vanishes upon heating to 50,000 K, cf. Figure 5b. This region of drastic composition changes is particularly difficult to treat with chemical models. In contrast, QMC simulations allow for an unbiased first-principles approach to these interesting phenomena. The lower row of the figure corresponds to extreme densities in the range of 10^{25} cm^{-3} and 10^{27} cm^{-3} which is of relevance for dwarf stars. Here no bound states exist because the electrons are in a strongly degenerate Fermi gas state. In contrast, the protons are still classical, but their Coulomb coupling parameter is much larger than one. The two lower figures indicate the formation, upon compression, of an ion liquid (Figure 5c) and an ion crystal that is embedded into a nearly ideal electron Fermi gas. This phenomenon was studied in more detail with PIMC simulations combined with the Kelbg potential in References [39, 40].

The PIMC simulations revealed that this approach is computationally very challenging. The first problem is the need to use increasingly large numbers of high-temperature factors when the temperature is lowered. However, the fundamental problem in the simulations of plasmas is the fermion sign problem (FSP) that arises from the need to use an anti-symmetrized density operator to correctly describe electrons. It was shown by Troyer and Wiese that the FSP is NP hard, cf. References [41, 42], which means there is an exponential increase in the computational effort when the particle number is increased or the temperature is lowered. This limits the simulations shown in Figure 5 to moderate values of the degeneracy parameter (not too low temperatures). In the meantime, more advanced PIMC concepts have been developed that will be briefly discussed in Section 4.5.

4.2 | Color Kelbg potential for PIMC simulations of the quark-gluon plasma

It had been noticed for a long time that there exist many qualitative similarities between the equilibrium phase diagram of a QGP and a partially ionized quantum plasma. This has led to the idea to transfer simulation methods that were developed for Coulomb systems to the QGP. In particular, V. Filinov and V.E. Fortov had the idea to apply PIMC simulations, which have proven successful for dense hydrogen (cf. Section 4.1), to the QGP. The goal was to investigate the confinement-deconfinement transition in the QGP that is expected to have taken place shortly after the Big Bang and was observed in laboratory experiments at the Relativistic Heavy Ion Collider (RHIC) and at CERN, and which has many similarities with the ionization/recombination transition in dense hydrogen plasmas. In fact, such PIMC simulations were presented by V. Filinov et al. in References [43–45] with the goal to avoid very expensive lattice QCD simulations. The main differences between the QCD case, compared to hydrogen plasma, are

1. the plasma constituents are quarks and anti-quarks (fermions) and gluons (bosons),
2. the quantum numbers are spin, flavour, and colour,
3. the quarks have comparable masses that depend on temperature and chemical potential,
4. the scalar electrical charge is replaced by a colour charge (SU(3) Wong vector),
5. a fully relativistic description is needed.

More details on the model and its justification can be found in References [43, 44]. Finally, the colour Kelbg potential has the form

$$\Phi_{ij}^{CK}\left(r;T,\mu_q\right)=\frac{g^2\left(T,\mu_q\right)}{4\pi}\frac{\left\langle Q_i|Q_j\right\rangle}{r}\left[1-e^{-r^2/\lambda_{ij}^2}+\frac{\sqrt{\pi}r}{\lambda_{ij}}\left(1-\mathrm{erf}\left[\frac{r}{\lambda_{ij}}\right]\right)\right], \tag{14}$$

where T is the temperature, μ_q the quark chemical potential, and g the coupling constant, whereas Q_i denotes Wong's quasiparticle colour variable (8D-vectors in the SU(3) group), and $\left\langle Q_i|Q_j\right\rangle$ denotes the expectation value of the scalar product of two colour vectors. Using the colour Kelbg potential (14) a path integral representation could be developed which involves the potential Φ^{CK} in the high-temperature factors. The thermodynamic results for the equation of state and density revealed good agreement with lattice QCD simulations. In addition, the colour PIMC simulations also yield in a straightforward way the pair distributions of the plasma constituents from which one could conclude about moderately coupled liquid-like behaviour and the existence of gluon bound states (glue balls) just below the confinement phase transition.

4.3 | Improved Kelbg potential

It has been noted long ago that the Kelbg potential is qualitatively very similar to the exact pair potential (the solution of the two-particle Bloch equation), even outside the validity range of perturbation theory. The largest differences occur at zero distance. While at zero distance the Kelbg potential has an incorrect value, its derivative is correct. This has led to the idea of improved quantum potentials, cf. References [46, 47] that contain a single additional parameter that maintains the correct derivative but can be adjusted such that also the value at zero can be "fixed," cf. References [6, 7]:

$$U_{ij}^{IK}\left(r;\gamma_{ij}\right)=\frac{e_ie_j}{r}\left[1-e^{-r^2/\lambda_{ij}^2}+\frac{\sqrt{\pi}r}{\lambda_{ij}\gamma_{ij}}\left(1-\mathrm{erf}\left[\frac{\gamma_{ij}r}{\lambda_{ij}}\right]\right)\right], \tag{15}$$

where $\gamma_{ij}=\gamma_{ij}(T)$ is a function of temperature. In the limit $T\to\infty$ the parameter approaches one, $\gamma_{ij}\to 1$, and $U_{ij}^{IK}\to V_{ij}^{K}$.

This potential is plotted in Figure 6 for a set of high temperatures (2.375Ha $\le T\le$ 19Ha) and compared to the standard Kelbg potential and the exact solution of the Bloch equation, cf. Reference [7]. At zero distance the improved Kelbg potential between an electron and an ion is significantly deeper than the standard Kelbg potential, whereas, for the case of two electrons, the trend is reversed.[7] Both, for the attractive electron-ion potential (Figure 6a) and its beta-derivative used in the thermodynamic estimator of the internal energy, cf. Reference [32], (Figure 6b), the improved Kelbg potential shows excellent agreement with the exact pair potential (the insets in the figures demonstrate their relative deviations)

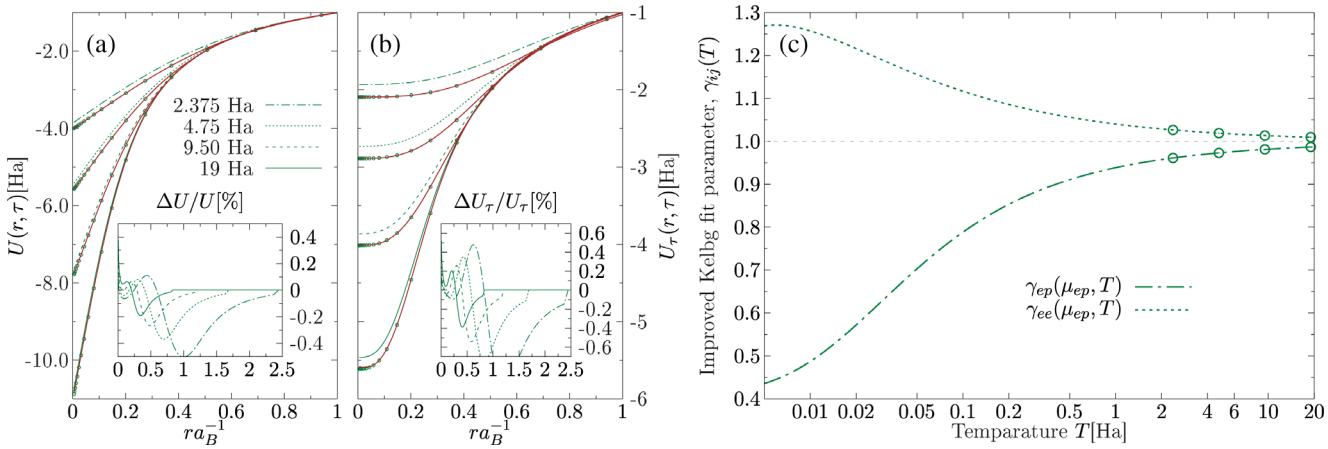

FIGURE 6 (a) Electron-proton quantum pair potential $U(r,\tau)$ and (b) Derivative with respect to the inverse temperature τ, $U_\tau(r,\tau)=\frac{d}{d\tau}[\tau\, U(r,\tau)]$. This expression contributes to the pair interaction energy and the internal energy, $E=-\frac{d}{d\beta}\ln Z$, where Z is the partition function. Both quantities are being used in the high-temperature factorization of the N-body density matrix, (Equation 12), with $\tau=\beta/P$, and are employed in the PIMC simulations of a dense hydrogen plasma in Figures 7–9. In the plot, the original "physical" temperature equals $T=62{,}250$ K (approximately 0.2 Ha). Using $P=12,24,48,96$ factors (curves from top to bottom), an effective high temperature, $\widetilde{T}=1/\tau=P\cdot T$, (specified in Hartree) is reached that is indicated by the values in the inset of (a). Different (coloured) curves correspond to three models: the Kelbg potential U^{K} (dashed green), the improved Kelbg potential U^{IK} (Equation 15, green dots) and the exact *pair potential* U^{PP} (Equation 3, solid brown curves) defined by the Slater sum of the electron-proton pair. The insets show the relative deviations between U^{IK} and U^{PP} and their corresponding β-derivatives. (c) The temperature-dependent fit parameter $\gamma\left(\mu_{ij},T\right)$ used in the improved Kelbg potential for a pair of electrons (ee) and for an electron-proton pair (ei), to reproduce the *pair potential* U^{PP}. The parameter γ is computed from the Padé fit of Reference [7]. The circles show the four temperature values used in panels (a) and (b).

over the entire range of pair distances. This is an impressive result considering that it is achieved with a single fit parameter γ.

The parameters γ_{ij} have been determined from the exact solution of the two-particle Bloch equation, cf. Reference [6], and the result is shown in Figure 6c. As discussed above, the γ-parameter converges to one in the high-temperature limit. The deviations start to be noticeable already for temperatures $T\sim 5\cdot 10^6$ K (see the $T=19$ Ha case in Figure 6a) which indicates the applicability range of the standard Kelbg potential that was derived in first-order perturbation theory with respect to the interaction strength. At lower temperatures, the γ_{ee}-parameter is monotonically increasing, whereas γ_{ep} decreases below one, cf. Figure 6c. The deviation from one reaches about 10% at $T\sim 150{,}000$ K (0.5Ha), and rapidly increases for lower temperatures, especially in the electron-proton case, due to the contribution of bound states in the Slater sum (3).

Let us consider again the value of the improved potential at zero distance which now replaces the previous result, Equation (7):

$$U_{ij}^{\mathrm{IK}}\left(r\to 0;\gamma_{ij}\right)=\frac{e_ie_j}{\lambda_{ij}(T)\gamma_{ij}(T)}=\frac{e_ie_j}{\lambda_{ij}^{\mathrm{eff}}(T)}\sim \mathrm{sign}\left(e_ie_j\right)\frac{T^{1/2}}{\gamma_{ij}(T)}. \tag{16}$$

This result shows that the parameter γ_{ij} has a simple interpretation: it represents the correction to the quantum extension of the particles due to interaction effects (deviations from the ideal gas limit). The effective extension is now $\lambda_{ij}^{\mathrm{eff}}(T)=\gamma_{ij}(T)\cdot\lambda_{ij}(T)$. From the behaviour displayed in Figure 6c, it is clear that $\lambda_{\mathrm{ep}}^{\mathrm{eff}}(T)\le\lambda_{\mathrm{ep}}(T)$, whereas $\lambda_{\mathrm{ee}}^{\mathrm{eff}}(T)\ge\lambda_{\mathrm{ee}}(T)$. Detailed investigations of the improved Kelbg potential can be found in References [6, 7].

4.4 | Use of the Kelbg potential and the improved Kelbg potential in semiclassical molecular dynamics simulations of quantum plasmas

The Kelbg potential and the improved Kelbg potential have been used not only in PIMC simulations but also in semi-classical MD simulations of dense hydrogen. The idea is that, since these potentials regularize the forces between plasma

particles at low separation, they correctly avoid the classical collapse of bound states of differently charged particles. Moreover, in the case of charge separation in an electric field, quantum effects captured by the Kelbg potential should reduce the restoring force. This was indeed observed in MD simulations of dense hydrogen. The density autocorrelation function and the dynamic structure factor and, from it, the plasmon dispersion of quantum degenerate electrons were computed in References [28, 48]. There it was observed that the optical plasmon dispersion, $\omega(k)$, increases slower with the wave number if quantum diffraction effects are taken into account. Similar Kelbg-potential-based MD simulations of correlation functions and transport properties were reported in Reference [49].

Semiclassical MD simulations were improved further by using the improved Kelbg potential, Equation (15). Applications to dense hydrogen revealed that the thermodynamic properties and pair distributions known from PIMC simulations can be reproduced very accurately by averaging over semiclassical trajectories, including the formation of atoms, see Reference [7]. These simulations broke down only with the onset of molecule formation, below $T \sim 50{,}000$ K. To apply semiclassical MD to the molecular region, an extension of the improved Kelbg potential to three-and four-particle effects would be required.

4.5 | New PIMC results for partially ionized hydrogen

The fermion sign problem in QMC simulations that was mentioned in Section 4.1 has been the subject of intense investigations. Even though no general solutions have been found so far, various strategies to avoid the problem have been presented. One is the development of restricted PIMC (RPIMC) simulations by Ceperley and co-workers, for example, References [50, 51]. While this has allowed the authors to eliminate the FSP formally, this procedure introduces uncontrolled errors, in particular, at finite temperatures. An alternative approach was developed in the group of one of the authors (M. Bonitz): PIMC simulations can be extended into the region of strong degeneracy and weak coupling that are not accessible to standard PIMC if, instead of the coordinate representation, PIMC is reformulated in second quantization. This novel approach was termed configuration PIMC (CPIMC) and was presented in Reference [52]. It could be confirmed for a degenerate electron gas that CPIMC does not have a sign problem at high density and accurately produces the thermodynamic properties of the moderately coupled electron gas at finite temperature, for example, Reference [53]. The next step was to combine CPIMC simulations with permutation-blocking PIMC—a substantially improved coordinate-space variant of PIMC developed by T. Dornheim, cf. Reference [54]. Combination of CPIMC and PB-PIMC,[55, 56] indeed, allowed one to avoid the FSP for the warm dense uniform electron gas (UEG) for all temperatures above one-half of the Fermi temperature. These results could be connected to the known ground state data in Reference [57] and yielded the first ab initio thermodynamic results for the UEG in the entire warm dense matter range, for example, Reference [58, 59].

The idea of PB-PIMC was recently extended by A. Filinov further to the grand canonical ensemble in Reference [23]. These novel fermionic propagator PIMC (FP-PIMC) simulations proved very accurate and efficient for the warm dense UEG. This was the basis to apply these novel PIMC simulations, combined with the improved Kelbg potential, again, to dense hydrogen with the hope of more accurate results than before (cf. the discussion in Section 4.1), without resorting to the fixed node approximation. First FP-PIMC results for the ion-ion PDF and the electron-ion PDF are shown in Figures 7 and 8 for a dense hydrogen plasma at $r_s = 7$ and two temperatures, $T = 31{,}250$ K and $T = 62{,}500$ K. Let us briefly discuss these results and the behaviour of the (improved) Kelbg potential in the simulations. At $T = 31{,}250$ K, (Figure 7a) one clearly observes the onset of molecule formation, manifest by the broad peak of $g^{ii}(r)$ around $r \sim 1.4a_B$. A cluster analysis of the PIMC data, similar to the one presented in Reference [60], reveals the following plasma composition: $x_H \sim 60\%$, $x_{H_2} \sim 2\%$ and $x_{H_2^+} \sim 1\%$, with x_a being the fraction of atoms, molecules and molecular ions, respectively. Increasing the temperature to 62,500 K (Figure 8) leads to thermal dissociation of the molecules and a reduction of the atom fraction by approximately a factor 2: $x_H \sim 28\%$, $x_{H_2} \sim 0.4\%$ and $x_{H_2^+} \sim 0.8\%$. Interestingly, this reduction of the atom fraction, directly correlates with a similar scaling (by a factor two) of the height of the peak of the electron-proton radial distribution function, $r^2 g^{ei}(r)$ around $r \sim a_B$, cf. Figures 7b and 8b.

We underline that these can be considered exact results (within statistical errors) which crucially depend on the use of the proper pair potentials and on the number P of high-temperature factors in the PIMC simulations. Therefore, in the following, we analyse the convergence of the present results with respect to the number of high-temperature factors, for $12 \leq P \leq 96$, for three quantum potentials: the Kelbg potential, U^{K}, the improved Kelbg potential, U^{IK}, and also the exact (off-diagonal) pair potential, U^{PP}. In the two right (left) panels of Figures 7 and 8 the P-convergence of the pair distributions is shown for the case of the (improved) Kelbg potential, cf. the green lines. For reference, we also show the P-convergence for the case of the exact potential U^{PP} (brown curves). Similarly, we display the P-convergence for several

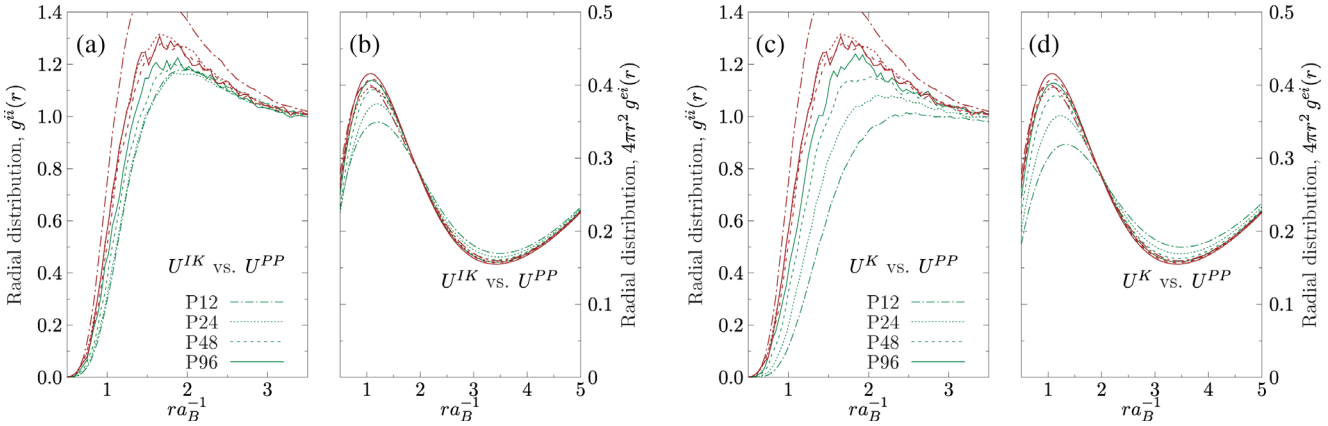

FIGURE 7 Convergence tests of PIMC simulations with respect to the number of high-temperature factors P. (a) and (c): Ion-ion PDF, $g^{ii}(r)$. (b) and (d): Electron-ion PDF, $r^2 g^{ei}(r)$ of dense hydrogen, for $r_s = \bar{r}/a_B = 7$ and temperature $T = 31{,}250$ K. The two left (right) panels correspond to simulations with the improved (original) Kelbg potential. Both cases are compared to the exact electron-ion pair potential, U^{PP}, cf. Equation (3), which already delivers converged results for $P \gtrsim 24$ (see the brown curves). The simulations are performed with the FP-PIMC approach, of Reference [23], which is generalized to two-component systems.

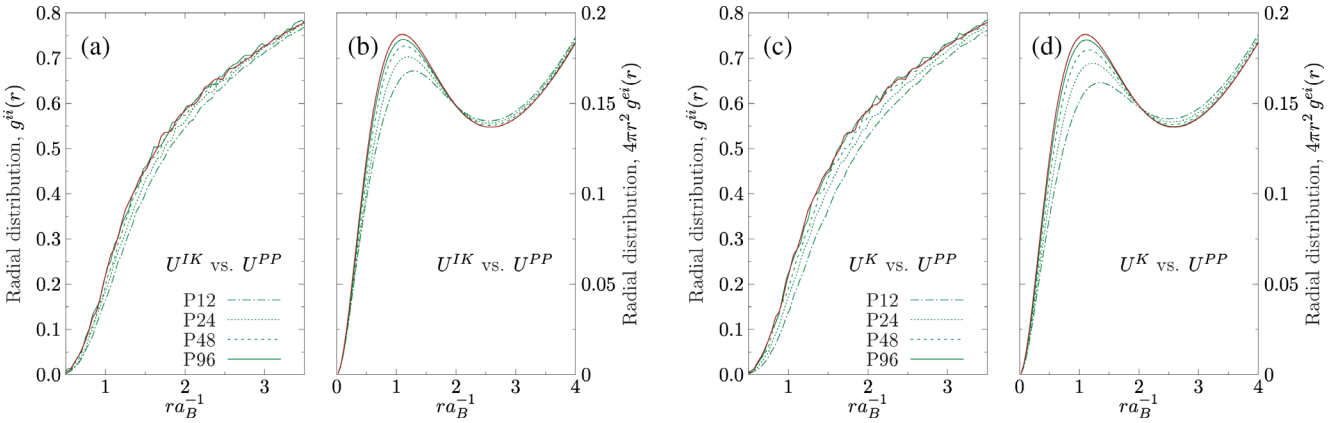

FIGURE 8 Same as in Figure 7 but for a twice as high temperature, $T = 62{,}500$ K. The results with U^{PP} are shown only for $P = 24$ (solid brown curve). The P-convergence of the results obtained with, both, the Kelbg potentials and the improved Kelbg potential is significantly faster than in Figure 7 and, again, the latter achieves a given accuracy at a significantly lower value P than the former.

thermodynamic functions of the hydrogen plasma at $r_s = 7$ and $T = 31{,}250$ K in Figure 9—including the internal energy and the pressure.

The present comparisons allow us to draw several important conclusions about the use of quantum potentials in PIMC simulations which are expected to hold for other $\{r_s, T\}$ combinations as well. At the first place, the substitution of the divergent electron-proton Coulomb potential with an effective one that includes quantum diffraction effects, makes quantum Monte Carlo simulations feasible and efficient, even at relatively low temperatures when the plasma composition is dominated by bound states. At $T = 31{,}250$ K, the convergence of the improved Kelbg potential with P is rather slow. On the other hand, the regular Kelbg potential converges significantly slower. Already at a twice as high temperature, both potentials exhibit a much faster convergence where, again, the improved Kelbg potential shows superior behaviour. The reason for the slow convergence is mainly the need to account for the non-isotropic (angle-dependent) correlation effects in the density matrix when an electron resides in close vicinity of an attractive Coulomb center, for details, see the discussion in Reference [6]. In this case, the use of the anisotropic exact pair potential is much more efficient, as can be seen from the faster convergence with P (see the brown curves). The contribution of such anisotropic configurations to the partition function, however, becomes significantly less relevant with increasing temperature, and becomes negligible when T becomes comparable to or exceeds the binding energy, that is, $T \gtrsim 150{,}000$ K (~1 Ry). In this case, the use

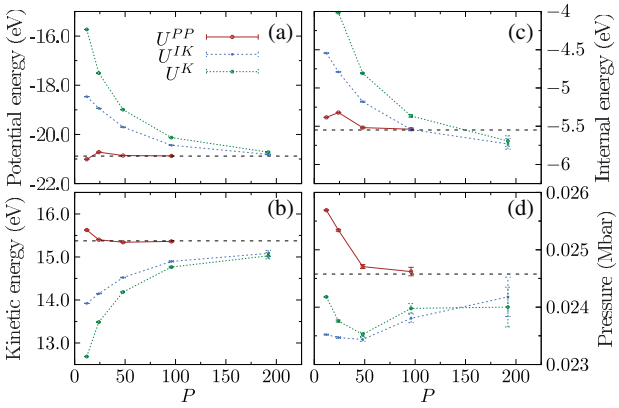

FIGURE 9 Convergence of thermodynamic functions obtained with FP-PIMC simulations with the number P of high-temperature factors, for $r_s = 7$ and $T = 31{,}250$ K and a system size of $N_i = N_e = 14$. (a) Potential energy; (b) kinetic energy; (c) total (internal) energy, and (d) pressure. The extrapolation to the $P \to \infty$ limit is indicated by the dashed lines. The simulations with the exact off-diagonal electron-ion pair potential $U^{\mathrm{PP}}(\mathbf{r}_1, \mathbf{r}_2)$ are compared to the improved (U^{IK}) and the original Kelbg (U^{K}) potential in the diagonal approximation, $U_{ep}(\mathbf{r}_1, \mathbf{r}_2) \approx 1/2\left[U_{ep}(\mathbf{r}_1\mathbf{r}_1) + U_{ep}(\mathbf{r}_2, \mathbf{r}_2)\right]$, to the binary Slater sum, cf. Equation (2), see also Reference [7].

of the improved Kelbg potential with the γ-fit parameter (cf. Figure 6c) becomes very advantageous and accurate PIMC simulations can be performed with a managable number of high-temperature factors.

5 | SUMMARY AND DISCUSSION

We have given a brief summary on the work of Günter Kelbg in the field of quantum plasmas. 60 years after his derivation of a regularized Coulomb potential that carries his name, these results still turn out to be useful. First, the Kelbg potential is a valuable analytical representation of the exact quantum mechanical potential, in the weak coupling limit, reflecting the temperature dependence of the interaction between two particles that arises from quantum diffraction and exchange effects. Moreover, this potential and the improved Kelbg potential have found and continue to find extensive use in MD and PIMC simulations of dense quantum plasmas. The Kelbg potential is also useful to benchmark improved semiclassical simulations such as wave packet MD, for example, Reference [61]. While effective quantum potentials have been derived by many authors, including C. Deutsch and co-workers, for example,[18,19,62] in contrast to the Kelbg potential, many of these do not fulfil the cusp condition (correct value of the derivative of the pair distribution function $g(r)$ at $r \to 0$) which is important for thermodynamic consistency of the results, for example, Reference [63]. As we have shown above, in addition to the correct derivative, also the correct absolute value $g(0)$ can be restored with the improved Kelbg potential. This value is important for many properties of the plasma, most importantly for the shape of the momentum distribution, $n(k)$. In a one-component Coulomb system, interaction effects lead to a power law decay $\lim_{k\to\infty} n(k) = Ck^{-8}$, for example,[64] instead of the exponential decay of the ideal gas Fermi function. Interestingly, the coefficient C is directly proportional to the on-top pair distribution function, $g^{\uparrow\downarrow}(0)$, that is, the PDF of opposite spin electrons, for example,[65,66] This behaviour could recently be confirmed over a broad density-temperature range by a combination of CPIMC and PIMC simulations.[67,68] The (improved) Kelbg potential should allow one to further extend this analysis to two-component plasmas.

ACKNOWLEDGMENTS

M. Bonitz acknowledges support by the Deutsche Forschungsgemeinschaft via grant BO1366/15-1. Open Access funding enabled and organized by Projekt DEAL.

DATA AVAILABILITY STATEMENT

The data that support the findings of this study are available from the corresponding author upon reasonable request.

REFERENCES

[1] F. Graziani, M. P. Desjarlais, R. Redmer, S. B. Trickey, Frontiers and Challenges in Warm Dense Matter, Springer, Cham **2014**.
[2] V. E. Fortov, Extreme States of Matter, Second ed., High Energy Density Physics, Springer, Heidelberg **2016**.
[3] E. I. Moses, R. N. Boyd, B. A. Remington, C. J. Keane, R. Al-Ayat, *Phys. Plasmas* **2009**, *16*(4), 041006.
[4] M. Bonitz, T. Dornheim, Zh. A. Moldabekov, S. Zhang, P. Hamann, H. Kählert, A. Filinov, K. Ramakrishna, J. Vorberger, *Phys. Plasmas* **2020**, *27*(4), 042710.
[5] Zh. A. Moldabekov, M. Bonitz, T. S. Ramazanov, *Phys. Plasmas* **2018**, *25*(3), 031903.
[6] A. Filinov, M. Bonitz, W. Ebeling, *J. Phys. A: Math. Gen.* **2003**, *36*, 5957.
[7] A. V. Filinov, V. O. Golubnychiy, M. Bonitz, W. Ebeling, J. W. Dufty, *Phys. Rev. E* **2004**, *70*, 046411.
[8] H. Falkenhagen, M. Leist, G. Kelbg, *Annalen der Physik* **1952**, *11*, 51.
[9] H. Falkenhagen, G. Kelbg, *Zeitschrift für Physikalische Chemie* **1953**, *202*(1), 56.
[10] H. Falkenhagen, G. Kelbg, *Annalen der Physik* **1954**, *58*, 653.
[11] Th. Bornath, W.-D. Kraeft, R. Redmer, G. Röpke, M. Schlanges, W. Ebeling, M. Bonitz, *Contrib. Plasma Phys.* **2017**, *57*(10), 434.
[12] G. Kelbg, *Annalen der Physik* **1964**, *468*(7–8), 385.
[13] G. Kelbg, *Annalen der Physik* **1963**, *467*(3–4), 219.
[14] G. Kelbg, *Annalen der Physik* **1963**, *467*(7–8), 354.
[15] G. Kelbg, *Annalen der Physik* **1964**, *469*(7–8), 394.
[16] H. J. Hoffmann, W. Ebeling, *Beiträge aus der Plasmaphysik* **1968**, *8*(1), 43.
[17] C. Deutsch, M. Lavaud, *Phys. Lett. A* **1972**, *39*(4), 253.
[18] C. Deutsch, M. M. Gombert, H. Minoo, *Phys. Lett. A* **1978**, *66*(5), 381.
[19] H. Minoo, M. M. Gombert, C. Deutsch, *Phys. Rev. A* **1981**, *23*, 924.
[20] H. J. Hoffmann, G. Kelbg, *Ann. Physik* **1966**, *17*, 356.
[21] W. D. Kraeft, D. Kremp, W. Ebeling, G. Röpke, Quantum Statistics of Charged Particle Systems, Akademieverlag, Berlin **1986**.
[22] W. Ebeling, H. J. Hoffmann, G. Kelbg, *Beiträge aus der Plasmaphysik* **1967**, *7*(3), 233.
[23] A. Filinov, P. R. Levashov, M. Bonitz, *Contrib. Plasma Phys.* **2021**, *61*(10), e202100112.
[24] J. Ortner, I. Valuev, W. Ebeling, *Contrib. Plasma Phys.* **1999**, *39*, 311.
[25] W. Ebeling, G. Röpke, *Plasma* **2023**, *6*(1), 1.
[26] V. S. Filinov, M. Bonitz, W. Ebeling, V. E. Fortov, *Plasma Phys. Control. Fusion* **2001**, *43*(6), 743.
[27] G. S. Demyanov, P. R. Levashov, *Contrib. Plasma Phys.* **2022**, *62*(10), e202200100.
[28] V. Golubnychiy, M. Bonitz, D. Kremp, M. Schlanges, *Phys. Rev. E* **2001**, *64*, 016409.
[29] W. Ebeling, A. Filinov, M. Bonitz, V. Filinov, T. Pohl, *J. Phys. A: Math. Gen.* **2006**, *39*(17), 4309.
[30] T. S. Ramazanov, Zh. A. Moldabekov, M. T. Gabdullin, *Phys. Rev. E* **2015**, *92*, 023104.
[31] S. Nagel, H. Stein, I. Leike, R. Redmer, G. Ropke, *J. Phys. B: Atomic Mol. Optic. Phys.* **1992**, *25*(3), 613.
[32] V. E. Fortov, V. S. Filinov, M. Bonitz, *JETP Lett.* **2000**, *72*, 244.
[33] V. S. Filinov, V. E. Fortov, M. Bonitz, P. R. Levashov, *JETP Lett.* **2001**, *74*, 384.
[34] V. S. Filinov, V. E. Fortov, M. Bonitz, D. Kremp, *Phys. Lett. A* **2000**, *274*(5), 228.
[35] S. A. Trigger, W. Ebeling, V. S. Filinov, V. E. Fortov, M. Bonitz, *J. Exp. Theoretic. Phys.* **2003**, *96*(3), 465.
[36] V. Filinov, P. Thomas, I. Varga, T. Meier, M. Bonitz, V. Fortov, S. W. Koch, *Phys. Rev. B* **2002**, *65*, 165124.
[37] V. Filinov, M. Bonitz, P. Levashov, V. Fortov, W. Ebeling, M. Schlanges, *Contrib. Plasma Phys.* **2003**, *43*(5–6), 290.
[38] V. S. Filinov, P. R. Levashov, M. Bonitz, V. E. Fortov, *Contrib. Plasma Phys.* **2005**, *45*(3–4), 258.
[39] M. Bonitz, V. S. Filinov, V. E. Fortov, P. R. Levashov, H. Fehske, *J. Phys. A: Math. Gen.* **2006**, *39*(17), 4717.
[40] M. Bonitz, V. S. Filinov, V. E. Fortov, P. R. Levashov, H. Fehske, *Phys. Rev. Lett.* **2005**, *95*, 235006.
[41] M. Troyer, U.-J. Wiese, *Phys. Rev. Lett.* **2005**, *94*, 170201.
[42] T. Dornheim, *J. Phys. A Mathematic. Theoretic.* **2021**, *54*(33), 335001.
[43] V. S. Filinov, Yu. B. Ivanov, V. E. Fortov, M. Bonitz, P. R. Levashov, *Phys. Rev. C* **2013**, *87*, 035207.
[44] V. S. Filinov, M. Bonitz, Y. B. Ivanov, E.-M. Ilgenfritz, V. E. Fortov, *Contrib. Plasma Phys.* **2015**, *55*(2–3), 203.
[45] V. S. Filinov, M. Bonitz, Y. B. Ivanov, E.-M. Ilgenfritz, V. E. Fortov, *Plasma Phys. Controll. Fusion* **2015**, *57*(4), 044004.
[46] M.-M. Gombert, H. Minoo, *Contrib. Plasma Phys.* **1989**, *29*(4–5), 355.
[47] H. Wagenknecht, W. Ebeling, A. Förster, *Contrib. Plasma Phys.* **2001**, *41*(1), 15.
[48] V. Golubnychiy, M. Bonitz, D. Kremp, M. Schlanges, *Contrib. Plasma Phys.* **2002**, *42*(1), 37.
[49] I. Morozov, H. Reinholz, G. Röpke, A. Wierling, G. Zwicknagel, *Phys. Rev. E* **2005**, *71*, 066408.
[50] D. M. Ceperley, *J. Statistic. Phys.* **1991**, *63*(5), 1237.
[51] S. X. Hu, B. Militzer, V. N. Goncharov, S. Skupsky, *Phys. Rev. B* **2011**, *84*, 224109.
[52] T. Schoof, M. Bonitz, A. Filinov, D. Hochstuhl, J. W. Dufty, *Contrib. Plasma Phys.* **2011**, *84*, 687.
[53] T. Schoof, S. Groth, J. Vorberger, M. Bonitz, *Phys. Rev. Lett.* **2015**, *115*, 130402.
[54] T. Dornheim, S. Groth, A. Filinov, M. Bonitz, *New J. Phys.* **2015**, *17*(7), 073017.
[55] T. Dornheim, S. Groth, T. Schoof, C. Hann, M. Bonitz, *Phys. Rev. B* **2016**, *93*, 205134.
[56] S. Groth, T. Schoof, T. Dornheim, M. Bonitz, *Phys. Rev. B* **2016**, *93*, 085102.
[57] S. Groth, T. Dornheim, T. Sjostrom, F. D. Malone, W. M. C. Foulkes, M. Bonitz, *Phys. Rev. Lett.* **2017**, *119*, 135001.
[58] T. Dornheim, S. Groth, T. Sjostrom, F. D. Malone, W. M. C. Foulkes, M. Bonitz, *Phys. Rev. Lett.* **2016**, *117*, 156403.

[59] T. Dornheim, S. Groth, M. Bonitz, *Phys. Rep.* **2018**, *744*, 1.
[60] B. Militzer, D. M. Ceperley, *Phys. Rev. E* **2001**, *63*, 066404.
[61] I. V. Morozov, I. A. Valuev, *J. Phys. A Mathematic. Theoretic.* **2009**, *42*(21), 214044.
[62] C. Deutsch, M. Lavaud, *Phys. Lett. A* **1973**, *39A*, 293.
[63] A. E. Carlsson, N. W. Ashcroft, *Phys. Rev. B* **1982**, *25*, 3474.
[64] V. M. Galitskii, V. V. Yakimets, *Soviet Physics JETP* **1967**, *24*, 3.
[65] H. Yasuhara, Y. Kawazoe, *Phys. A Statistic. Mech. Appl.* **1976**, *85*(2), 416.
[66] J. C. Kimball, *J. Phys. A Mathematic. Gen.* **1975**, *8*(9), 1513.
[67] K. Hunger, T. Schoof, T. Dornheim, M. Bonitz, A. Filinov, *Phys. Rev. E* **2021**, *103*, 053204.
[68] T. Dornheim, J. Vorberger, B. Militzer, Z. A. Moldabekov, *Phys. Rev. E* **2021**, *104*, 055206.

How to cite this article: M. Bonitz, W. Ebeling, A. Filinov, W. Kraeft, R. Redmer, G. Röpke, *Contrib. Plasma Phys*. **2023**, *63*(3-4), e202300029. https://doi.org/10.1002/ctpp.202300029